Biochimica et Biophysica Acta 1841 (2014) 1700–1708

Contents lists available at ScienceDirect

Biochimica et Biophysica Acta

journal homepage: www.elsevier.com/locate/bbalip

One precursor, three apolipoproteins: The relationship between two crustacean lipoproteins, the large discoidal lipoprotein and the high density lipoprotein/β-glucan binding protein

Stefanie Stieb [a], Ziv Roth [b], Christina Dal Magro [a], Sabine Fischer [c], Eric Butz [a], Amir Sagi [b], Isam Khalaila [d], Bernhard Lieb [a], Sven Schenk [a,1], Ulrich Hoeger [a,*]

[a] Institute of Zoology, Johannes Gutenberg-University, D-55099 Mainz, Germany
[b] Department of Life Sciences and the National Institute for Biotechnology in the Negev, Ben Gurion University, Beer Sheva 84105, Israel
[c] Institute of Molecular Genetics, Johannes Gutenberg-University, D-55099 Mainz, Germany
[d] Department of Biotechnological Engineering, Ben Gurion University, Beer Sheva 84105, Israel

ARTICLE INFO

Article history:
Received 5 June 2014
Received in revised form 19 September 2014
Accepted 24 September 2014
Available online 2 October 2014

Keywords:
Discoidal lipoprotein
High density lipoprotein/β-glucan binding protein
Lipoprotein precursor
Transcriptome analysis
Crustacea

ABSTRACT

The novel discoidal lipoprotein (dLp) recently detected in the crayfish, differs from other crustacean lipoproteins in its large size, apoprotein composition and high lipid binding capacity. We identified the dLp sequence by transcriptome analyses of the hepatopancreas and mass spectrometry. Further de novo assembly of the NGS data followed by BLAST searches using the sequence of the high density lipoprotein/β-glucan binding protein (HDL–BGBP) of *Astacus leptodactylus* as query revealed a putative precursor molecule with an open reading frame of 14.7 kb and a deduced primary structure of 4889 amino acids. The presence of an N-terminal lipid binding domain and a DUF 1943 domain suggests the relationship with the large lipid transfer proteins. Two putative dibasic furin cleavage sites were identified bordering the sequence of the HDL–BGBP. When subjected to mass spectroscopic analyses, tryptic peptides of the large apoprotein of dLp matched the N-terminal part of the precursor, while the peptides obtained for its small apoprotein matched the C-terminal part. Repeating the analysis in the prawn *Macrobrachium rosenbergii* revealed a similar protein with identical domain architecture suggesting that our findings do not represent an isolated instance.

Our results indicate that the above three apolipoproteins (i.e HDL–BGBP and both the large and the small subunit of dLp) are translated as a large precursor. Cleavage at the furin type sites releases two subunits forming a heterodimeric dLP particle, while the remaining part forms an HDL–BGBP whose relationship with other lipoproteins as well as specific functions are yet to be elucidated.

1. Introduction

The transport of hydrophobic lipids through hydrophilic, aqueous physiological fluids requires the presence of lipoprotein-amphiphilic molecules acting as mediators between these two phases. While vertebrates rely upon a variety of lipoproteins with various lipid and apoprotein compositions [1], many invertebrates possess only one type of sex-independent-lipoprotein, such as the lipophorins in flying insects and chelicerates [2–4] or the discoidal lipoprotein from the polychaete *Nereis virens* [5]. Lipoproteins can arise in different density classes depending on the species or the physiological state and may serve not only for transport of lipids, but also for hemolymph clotting and wound closure as shown at least for insect and crustacean lipoproteins as outlined below [6–8]. With respect to the sex unspecific lipoproteins, two types are known in the crustaceans: the clotting proteins (CP), belonging to the very high density lipoproteins (VHDL's) and the high density lipoproteins/β-glucan binding proteins (HDL–BGBPs). The HDL–BGBPs are the main lipid transporting proteins containing about 50% bound lipids mainly in the form of phospholipids and represent a HDL type with buoyant densities between 1.08 and 1.22 g/ml [6,9–14]. The CP's serve for hemolymph clotting (due to polymer formation catalyzed by a hemocyte derived enzyme, transglutaminase, E.C. 2.3.2.13) and thus initiate wound closure [6]. The HDL–BGBPs on the other hand, besides their role in lipid transport, have a binding site for β-glucans of microbial origin; they serve for antimicrobial defense and act together with the hemocytes [6,7,12,15–18]. After binding of microbial or fungal β-1,3 glucans, HDL–BGBP is phagocytized by hemocytes as the other main component of the innate immune system [19].

Abbreviations: CP, clotting protein; dLp, discoidal lipoprotein; HDL–BGBP, high density lipoprotein/β-glucan binding protein; LP–BGBP, lipopolysaccharide and β-glucan binding protein; (V)HDL, (very) high density lipoprotein.

* Corresponding author. Tel.: +49 6131 39 22881; fax: +49 6131 39 23835.
E-mail address: uhoeger@uni-mainz.de (U. Hoeger).
[1] Present address: Max F. Perutz Laboratories, University of Vienna, 1030 Wien, Austria.

http://dx.doi.org/10.1016/j.bbalip.2014.09.020
1388-1981/

The β-glucan binding properties of the HDL–BGBPs are shared with yet another group of proteins designated lipopolysaccharide and β-glucan binding proteins (LP–BGBPs). The LP–BGBP group of proteins lacks a lipid binding domain. Both groups are sometimes simply termed β-glucan binding proteins in the literature and in database entries, although their constituting apoproteins have clearly different molecular masses around 50 kDa (LP–BGBPs) and 105–110 kDa (HDL–BGBPs), respectively. Therefore, the term HDL–BGBP will be used here throughout for clarity. In phylograms, the LP–BGBPs form a clade different from the BGBPs [20]. The LP–BGBPs of a number of species have been described and characterized on the molecular level ([21] and cited references); in contrast, molecular data for HDL–BGBP exist only for four species (*Pacifastacus leniusculus*, GenBank: CAA56703.1; *Litopenaeus vanamei*, AAO92933.1; *Fenneropenaeus chinensis*, ADW10720.1; *Astacus leptodactylus*, CAX65684). While recent molecular analyses have established a relationship of the LP–BGBP with glucanases [22], the relationship of the HDL–BGBPs with other lipoproteins is less clear. A glucanase like stretch has been assumed in the HDL–BGBP of the signal crayfish *P. leniusculus*, [23] but to date, a BLAST search using the known HDL–BGBP sequences (see above) does not reveal any clues for a relationship neither with the LP–BGBPs nor with other known lipoproteins, as noted earlier [24]. This raises the possibility that the crustacean HDL–BGBP represents an independent group of multifunctional proteins.

In contrast, the recently discovered discoidal lipoprotein is also a high density lipoprotein (buoyant density of 1.10 g/ml) and has been described as a heterodimer with two apoproteins of 80 and 240 kDa and a high lipid content of 70–80% [14]. It differs from the HDL–BGBP in its large discoidal shape with a diameter of 40 nm while the HDL–BGBPs are smaller (13 nm in diameter) but can also be discoidal [9]. So far, large discoidal lipoproteins have been reported before only in one species of crayfish, *A. leptodactylus* [14] and in another invertebrate, the polychaete *N. virens* [5] but not in other invertebrates or vertebrates. Discoidal lipoproteins such as the nascent human HDL containing the type A apolipoproteins are smaller [25] and represent transient particles that mature by the acquisition of cholesteryl esters [26,27]. The recent discovery of the dLp in the crayfish *A. leptodactylus* has raised the question as to its physiological function since it has been found to be absent in the congener, *Astacus astacus* [14]. Analysis of the hemolymph of various other decapods using the same isolation technique has also revealed the absence of the dLp in the hemolymph (Schenk, Stieb, Hoeger, unpublished results).

To elucidate the structure of this new discoidal lipoprotein, preliminary LC–MS analyses of the two apoproteins of the dLp were carried out (Roth, unpublished) revealing the presence of peptides matching those found in the sequences of the HDL–BGBP of *P. leniusculus* and *A. leptodactylus* published previously. This indicated a relationship of the HDL–BGBP and the dLp. The present study was therefore initiated to further explore the structure of this unusual lipoprotein and its relationship with other known crustacean lipoproteins. Here, we show by the combination of molecular, transcriptome and mass spectroscopic analysis that both dLp and HDL–BGBP arise from a common precursor which can give rise to the distinct mature proteins after proteolytic cleavage.

2. Material and methods

2.1. Animals

A. leptodactylus (36–75 g fresh weight, carapace length 56–68 mm) were obtained from Edelfish GmbH, Frankfurt, Germany. *A. astacus* of similar size was obtained from Edelkrebszucht Stiftlandkrebse, Tirschenreuth, Germany. The crayfish were kept at 18–20 °C in 40 l plastic trays in recirculated freshwater and fed pieces of frozen fish weekly. Adult *M. rosenbergii* were collected from the Aquaculture Research Station of the Ministry of Agriculture at Dor, Israel and held at Ben-Gurion University facility (27–28 °C, 12 h daylight, fed ad libitum). In all animals, intermolt stages were used.

2.2. Total RNA extraction, first strand cDNA synthesis and sequencing of a cDNA fragment of HDL–BGBP

The animals were anesthetized on ice for 30 min and killed by decapitation. The hepatopancreas was excised and total RNA was extracted from the hepatopancreas by the phenol–chloroform method [28] using TRI Reagent (Applied Biosystems) following the manufacturer instructions. 1 μg of RNA was used for the first strand cDNA synthesis using M-MLV reverse transcriptase (New England Biolabs) and the protocol given by the manufacturer. To amplify the HDL–BGBP cDNA fragment of *A. leptodactylus*, primers were designed (primer set I; see supplementary Table A1) using the online tools Oligo Calc and OligoAnalyzer 3.1 and the sequence for *P. leniusculus* (GenBank: CAA56703.1) as reference. Taq-Polymerase (New England Biolabs) was used according to the manufacturer instructions. The PCR was started with denaturation for 5 min at 95 °C, followed by 39 cycles consisting of a 1 min step at 95 °C, a 45 s annealing step with a variable temperature depending on the primer pair and a 1 min extension step at 72 °C. A final extension step followed for 10 min at 72 °C. The cDNA fragments were sequenced and assembled and the sequences were compared with other HDL–BGBPs using BLAST and sequence alignments were performed using Cobalt or ClustalW at the NCBI server (http://www.ncbi.nlm.nih.gov/).

2.3. Transcriptome analysis of the hepatopancreas, next generation sequencing and data processing to identify the dLp/HDL–BGBP precursor

Total RNA was extracted from the hepatopancreas of *A. leptodactylus* with QIAsymphony RNA Kit (Qiagen) according to the manufacturer instructions. Total RNA quality and quantity was checked using an Agilent Bioanalyzer 2100 and Nanodrop spectrophotometer. Poly A + RNA was isolated, fractionated and double stranded cDNA was synthesized using the TruSeq RNA sample prep v2 protocol (Illumina Inc., San Diego, CA). End-repaired, A-tailed and Adaptor-ligated cDNA was PCR-amplified by 12 cycles. The library was sequenced in paired-end mode (2 × 100 bp) using 1/4 lane of an Illumina HiSeq 2000 flowcell. NGS data analysis was performed using the software package CLC bio Genomics Workbench 6.0.1. Raw data were processed using several filters for sequence quality, ambiguous nucleotides and length. Low quality reads were trimmed with the modified-Mott trimming algorithm implemented in the workbench (quality limit 0.01). No ambiguous nucleotides were allowed in the sequence after trimming. Terminal nucleotides at both sequence ends were removed (15 nucleotides at 5′ end, 10 nucleotides at 3′ end). Resulting reads with a length shorter than 15 nucleotides were discarded. De novo assembly of trimmed reads was conducted with the following parameters: word size = 24, bubble size = 50, minimum contig length = 250, distance between paired reads = 150. Resulting de novo contigs were transformed into a database to identify sequences of interest through BLASTn searches using the HDL–BGBP sequence (see preceding section) as query.

To verify the sequence of the putative dLp/HDL–BGBP precursor obtained by the bioinformatic approach, total RNA was extracted from the hepatopancreas of *A. leptodactylus* using the peqGOLD Total RNA Kit (Peqlab) according to the manufacturer instructions. The quality and quantity of the isolated total RNA was checked using an Aligent Bioanalyzer 2100 and a Nanodrop spectrophotometer, respectively. The cDNA synthesis was carried out using the Maxima H Minus First Strand cDNA Synthesis Kit (Thermo) according to the manufacturer instructions. A set of 27 primer pairs (primer set II; see supplementary Table A2) was designed to cover the whole dLp/HDL–BGBP precursor sequence. For the amplification, a standard PCR with Taq-polymerase and touchdown-PCR program was performed to optimize the results (see supplementary Table A3). The PCR reactions were checked by

agarose gel electrophoresis. After purification of the PCR products with exonuclease I and shrimp alkaline phosphatase (SAP), Sanger sequencing was performed and the sequences were aligned with the dLp/HDL–BGBP precursor sequence identified by Illumina sequencing as reference.

The *M. rosenbergii BGBP* gene was found using tBLASTn searches using *A. leptodactylus* HDL–*BGBP* sequence against *M. rosenbergii* larval and post larval transcriptome libraries [29].

2.4. Mass spectrometry of the apoproteins of dLp and HDL–BGBP

Following gel electrophoresis, the apoprotein bands were visualized by Coomassie blue staining. The bands were cut out and prepared for in gel digestion as described before [30]. MS peptide analysis and tandem MS fragmentation were performed with an LTQ-Orbitrap spectrometer (Thermo Scientific), operated in the data-dependent mode to enable switching between MS and collision-induced dissociation tandem MS analyses of the top eight ions. Collision-induced dissociation fragmentation was performed at 35% collision energy with a 30 ms activation time. Proteins were identified and validated by using the SEQUEST algorithm in Proteome Discoverer 2.0 software (Thermo Scientific) using the deduced amino acid sequence obtained from Illumina sequencing. Mass tolerance for precursor and fragmentations were set to 10 ppm and 0.8 Da, respectively. Only high-confidence peptides were chosen (Xcorr > 2 and >2.5, for doubly and triply-charged species, respectively).

2.5. SDS PAGE and Western blotting

SDS-PAGE was carried out in Protean Mini® apparatus (BioRad) using 3.5% stacking/7.5% running gels. The gels were stained with Coomassie Blue and digitized using a standard flatbed scanner. The Java program Gelanalyzer (www.gelanalyzer.com) was used to calculate the apparent molecular mass of the peptides. To calculate the stoichiometry of the apoproteins, the relative densities of the apoproteins in each gel lane were measured as described [4] using Image J 1.46o (http://rsb.info.nih.gov/ij/).

For Western blotting, the separated proteins were transferred to nitrocellulose membranes for 90 min at 40 mA using the buffer system by Kyhse-Andersen [31]. The blot membranes were first blocked for 1 h in phosphate buffered saline (PBS) containing 5% skimmed milk powder, washed in PBS for 5 min, and then probed over night at 4 °C with diluted (1:7500 in PBS) antisera. After treatment with antiserum, the blot membrane was washed for five times with PBT and once with PBS. The blot was then incubated for 90 min with alkaline phosphatase-conjugated goat anti-rabbit IgG (Sigma) diluted 1:20,000 in PBS containing 1.25% skimmed milk powder. After three washes with PBT, the blots were washed with distilled water and finally developed in a staining solution containing 100 mM Tris, 100 mM NaCl, 50 mM $MgCl_2$, pH 9.0 with 0.03% 4-nitro blue tetrazolium chloride (NBT) and 0.015% 5-bromo-4-chloro-3-indolyl-phosphate (BCIP) as chromogens [32].

2.6. Hemolymph collection and lipoprotein isolation

For the isolation of lipoproteins, the hemolymph was collected from the arthrodial membrane using a 40 × 0.8 mm sterile syringe needles. The hemolymph drops were collected on ice into 15 ml Falcon type tubes containing 0.1 vol. of EDTA anticoagulant (50 mM EDTA, 225 mM NaCl, pH 7.4) and the samples were gently mixed immediately. Hemocytes were pelleted first for 1 min at 1000 ×*g* at 4 °C and the supernatant was recentrifuged for 10 min at 4500 ×*g* at 4 °C to further pellet cell debris. The clear supernatant was stored at −20 °C until further use. Lipoproteins were isolated by a two step KBr density gradient ultracentrifugation as described before [4].

2.7. ELISA measurements of dLp and HDL–BGBP titers in the hemolymph

Antisera against the *A. leptodactylus* dLp and BGBP were raised in rabbits using lipoproteins purified as described [14] and were obtained through Pineda Antibody Service (Berlin, Germany). Hemolymph was collected as above and the hemocytes were removed by centrifugation. The hemolymph was diluted by serial dilutions (2×10^4–3.2×10^5 fold) and 50 µl were used to coat the wells of a 96 well microplate (Sarstedt). After incubation for 1 h at 37 °C, the fluid was removed and the wells were blocked with 300 µl blocking buffer (0.1% BSA in PBS). After rinsing with 300 µl PBS, 50 µl of antiserum (diluted 1:1000) was added and the wells were incubated for 2 h at room temperature. The wells were washed for three times with 200 µl PBT (PBS containing 0.1% Tween 20). 50 µl of the secondary antibody (goat anti-rabbit, peroxidase coupled, SIGMA, 1:2500 in PBS/0.1% BSA) was added and the wells were further incubated for 1 h at room temperature. The wells were washed again (3 × 200 µl PBT) and 50 µl substrate solution (0.4 mg/ml o-phenylene diamine, 0.4 µl/ml of 30% H_2O_2 in 50 mM Na_2PO_4/25 mM Na-citrate, pH 5.0) was added. After color development, the reaction was stopped by the addition of 50 µl 1 N sulfuric acid and the plates were read at 490 nm. Standard curves (0.1–200 ng/well) were prepared with purified dLp and BGBP, respectively.

2.8. Immunohistochemistry

Crayfish were anesthetized on ice for 30 min and killed by decapitation. The hepatopancreas was excised, washed in phosphate buffered saline (PBS; 137 mM NaCl, 8 mM Na_2HPO_4, 3 mM KCl, 2 mM KH_2PO_4, pH 7.4) and fixed overnight in 4% paraformaldehyde/PBS. The fixed tissue was washed for three times in PBS and transferred sequentially to saccharose solutions of increasing concentrations (10, 20 and 30%) over two days at 4 °C. For the preparation of cryosections, the specimens were embedded in Tissue Tek (Richard-Allan-Scientific), placed on aluminum discs and frozen at −22 °C. Cryosections of 10 µm were cut on a Microm HM 560 Cryostat. The sections were transferred to polylysin coated slides and dried for at least 3 h. The dried sections were washed first for 5 min with PBT and blocked for 1 h with PBS containing 5% goat serum. After washing three times with PBS, the sections were incubated with the primary antibody (see above, antiserum diluted 1:5000) for 90 min at room temperature. The cells were washed again three times in PBS and then incubated for 1 h with the secondary antibody (goat anti rabbit conjugated either to Alexa 488 fluorophore, diluted 1:400; or to Atto 647 fluorophore, diluted 1:1000). After two washes with PBS, the sections were treated with PBS containing TRITC-Phalloidin (0.3 µg/ml PBS) and finally, after an additional wash with PBS, covered with embedding medium (2.5 mg/ml of diazabicyclo[2.2.2]octan in 10% PBS/90% glycerol containing 1 µg/ml of DAPI) prior to adding the coverslip. Dissociated hepatopancreas cells were prepared as described by Fiandra et al. [33]. The dissociated cells were fixed in 1% paraformaldehyde for 1 h, washed in PBS and treated with PBS containing 0.25% Tween-20 for 1 h. The subsequent steps were carried out as above. Images were acquired using a Leica DB6000 epifluorescence microscope using a 40x and 100x oil immersion lenses and the L5 filter cube. Stacks of 20–80 images were acquired using the Leica AS V2.1 software. The image stacks were deconvoluted by applying the blind deblur method and the deconvoluted images of each stack were combined to a single image plane applying the maximum intensity projection. For better visualization, the images were adjusted for brightness and contrast using Volocity LE (Improvision Ltd/PerkinElmer, Waltham, MA, available at http://www.cellularimaging.com).

2.9. Bioinformatic methods

Contig assembly of the reads obtained by Illumina sequencing was performed using software package CLC bio Genomics Workbench 6.0.1

(see above). The presence of furin cleavage sites in the deduced sequences was predicted using the online tool ProP (http://www.cbs.dtu.dk/services/ProP/); [34]. The presence of signal peptides was predicted using the SignalP 4.1 server (http://www.cbs.dtu.dk/services/SignalP/); [35]. BLAST search, identification of conserved domains and multiple alignments with ClustalW were performed using the server at the NCBI. For 3D modeling of the N-terminal lipid binding domain, the sequence of the first 1200 amino acids of the large dLp subunit was submitted to the Phyre2 server (http://www.sbg.bio.ic.ac.uk/phyre2/html/) [36].

3. Results

3.1. Sequencing of the HDL–BGBP gene of A. leptodactylus

Sequencing of the HDL–BGBP gene of *A. leptodactylus* using primer set I (supplementary Table A1) yielded a fragment of 4062 base pairs lacking start and stop codons with a deduced sequence of 1353 amino acids and a calculated molecular mass of 153 kDa. The nucleotide sequence was deposited at GenBank under the accession number FN298411.2. This sequence served to identify the full length dLp/HDL–BGBP precursor (see below). A BLAST search using the translated amino acid sequence revealed significant homology with three other crustacean HDL–BGBPs (*P. leniusculus*; GenBank: CAA56703.1, 89% Identity; *F. chinensis*, ADW10720.1, 54% identity and *L. vannamei*, P81182.2, 55% identity).

3.2. RNASeq and identification of the dLp–BGBP precursor

The above HDL–BGBP sequence was subjected to a BLAST search using the local database of *de novo* contigs obtained from the *A. leptodactylus* hepatopancreas by paired-end Illumina sequencing (see Methods section). Of 25,500 contigs generated, two contigs of 11.7 and 3.1 kb lengths were identified. By manually adjusting the distance between paired reads, these two contigs were combined resulting in an open reading frame of 14.7 kb enclosed in a 5′- and 3′-UTR. With a translated sequence of 4889 amino acids, a molecular mass of 546 kDa was calculated. The sequence was verified using cDNA synthesized from *A. leptodactylus* hepatopancreas mRNA with the primer set II (supplementary Table A2) followed by PCR amplification and direct Sanger sequencing. The translated amino acid sequence was used for a SignalP search and a BLAST search against the non-redundant protein database of the NCBI server to identify conserved domains. An N-terminal signal peptide was identified, followed by a lipoprotein N-terminal domain (SMART accession number 00638) which is also known as vitellogenin_N (Pfam accession number PF01347). In addition, two domains of unknown function (DUF 1943 and DUF 1081; accession numbers pfam06448 and pfam09172, respectively) were found (Fig. 1).

The presence of the lipoprotein N-terminal domain was confirmed by molecular modeling. On the basis of the lamprey lipovitellin (PDB 1LSH) as template, this domain was predicted with 100% confidence using the first 868 amino acid residues (72% of the submitted sequence; see supplementary Fig. B1).

In the central part of the amino acid sequence, two putative dibasic furin cleavage sites (with the motifs RAKR and RARR, respectively) were predicted by the ProP web server which were located adjacent to the sequence corresponding to the translated HDL–BGBP sequence (see above) with a length of 1108 amino acids and a calculated molecular mass of 126 kDa. Corresponding dibasic cleavage sites were also found in the HDL–BGBP sequences of *M. rosenbergii* and several other crustaceans (GenBank accession Nr. in parentheses): *A. astacus* (AHK23026), *P. leniusculus* (CAA56703.1), *F. chinensis* (AAO92933.1), *L. vanamei* (ADW10720.1) and in three translated EST sequences from *Homarus americanus* (EW703128.1), *Carcinus maenas* (DY656665.1) and *Petrolisthes bicinctus* (FE813732.1) as shown in Fig. 2.

The primer set II was further used to synthesisze cDNA from the hepatopancreas of a congener, *A. astacus*, with subsequent PCR amplification and Sanger sequencing as above. An almost identical translated sequence (98% identity) of the same length was obtained. The same domain structure was also found for the related sequence obtained from an NGS transcriptome library of the prawn *M. rosenbergii* [29, see

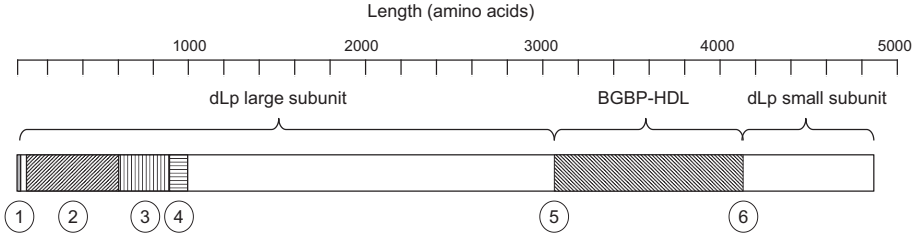

		A. leptodactylus			*M. rosenbergii*	
		Amino acid positions		Sequence coverage	Amino acid positions	Sequence coverage
1	Signal peptide	1 - 16	Large subunit	66%	1 - 17	not det.
2	N-terminal lipid binding domain	37-568			38-571	
3	Duf 1943 (Pfam 09172)	601-880			604-882	
4	Duf 1081 (Pfam 06448)	893-983			895-984	
5	End of large subunit, Furin cleavage site I	3047-3050 (RAKR)			3014-3016 (RPRR)	
5	Begin of BGBP-HDL	3051	BGBP-HDL	52%, 60% *)	3017	68%
6	End of BGBP-HDL, Furin cleavage site II	4155-4158 (RARR)			4112-4115 (RVKR)	
6	Begin of small subunit	4159	Small s-unit	63%	4116	not det.
	End of small subunit	4889			4583 (incomplete)	

Fig. 1. Schematic representation of the domains and their corresponding amino acid positions identified in the discoidal lipoprotein/high density lipoprotein–β-glucan binding protein precursor of *A. leptodactylus* and in the related protein of *M. rosenbergii*. The sequence coverage by the peptides obtained by the mass spectroscopic analysis is also given. *), two analyses were performed. not det., not determined.

```
                                  ← Begin HDL-BGBP
KF896205.1 Ast lept FGSLNRAKRSLEFKMMNDAGEASLVTNFNSAKLHLKTPFARAEEVTWEITKV 3101
KF956526.1 Ast ast  FGSLNRAKRSLEFKMMNDAGEASLVTNFNSAKLHLKTPFARAEEVTWEITKV 3101
CAA56703.1 Pac len  FGSLNRAKRSLEFKMMNDAGEASLVTNFNSAKLHLKTPFARAEEVTWEITKV  144
SRX445724  Mac ros  FGALNRPKRSLEFQMMSDDSAATFAANFNSLSMEVKTPFAAANQIKWEVVKV 3060
AAO92933.1 Lit van  FGSLNRSKRSLEMRMMNDAGQASLAGNFNSLRFNMKTPFERAEQISWEVTKT  232
ADW10720.1 Fen chin FGSLNRSKRSLEMRMMNDAGRASLAGNFNSLKFNIKTPFERAEQISWEITKT  240
EW703128.1 Hom am   ----------------------------------------------------
DY656665.1 Car mae  ----------------------------------------------------
FE813732.1 Pet bic  ----------------------------------------------------

                                              End HDL-BGBP →
KF896205.1 Ast lept EIELGEDDQEVEAHFTYNSEGVKARLSSPYTGDHSIRARRSIASDSFFTELG 4170
KF956526.1 Ast ast  EIELGEDDQEVEAHFTYNSEGVKARLSSPYTGDHSIRARRSIASDSFFTELG 4170
CAA56703.1 Pac len  EIELGEDDQEVEAHFTYNSEGVKARLNSPYTGDHSIRARRSIASDSFFTEIG 1218
SRX445724  Mac ros  IEELGGEG-EIEARIIYNAEGLQARLNSLRTGAHSIRVRRSISSDGFFAEAG 4130
AAO92933.1 Lit van  EIDLNENGQEVEATFFLDSEGIKARLSSAVLGDHSIRVRRSVAPDGFYAEAG 1303
ADW10720.1 Fen chin EIDLNENGQEVEATFFLDSEGIKARLTSTVLGDHSIRVRRSVSPDGFYAEAG 1304
EW703128.1 Hom am   DVELGQNGEKIEAEFVYDSEGVKARLTSPFTGQHTMRVRRSVSEQSFSAFAG   98
DY656665.1 Car mae  EAQLGSD-EHLEAEFKYNSDNVRARLMSPFTGEHRARARRSISSDSFFSEVS  122
FE813732.1 Pet bic  EAELGRDGQEVEAELVYNSDGVKARLSSPFTGRHSVRARRSISSDSFFSEIA  183
                      :*     .:** :  ::: ::*** *   * *  *.***:: :.* :* .
```

Fig. 2. Partial multiple alignment of the translated amino acid sequences of the high density lipoprotein/β-glucan binding protein of *A. leptodactylus* (GenBank KF896205.1), *A. astacus* (KF956526.1) and *M. rosenbergii* (SRX445724) with similar sequences of three other decapod crustaceans, *P. leniusculus* (Q26048), *F. chinensis* (ADW10720), *L. vanamei* (AAO92933) and three additional translated sequences found in the NCBI EST database for *H. americanus* (EW703128.1), *C. maenas* (DY656665.1) and *P. bicinctus* (FE813732.1). Two different sequence parts are shown containing two putative furin cleavage sites as predicted by the ProP online tool (squared boxes; bold letters). Asterisks and colons indicate identical amino acids and conservative replacements, respectively. The multiple alignments were carried out using ClustalW 2.1.

Fig. 2]. The nucleotide sequences were deposited at the GenBank database under the accession numbers KF896205, KF956526 and SRX445724.

3.3. Mass spectroscopic analysis of the discoidal lipoprotein of A. leptodactylus and the related protein of M. rosenbergii

In a previous study, the molecular masses of the two dLp apoproteins of *A. leptodactylus* were calculated from SDS-PAGE gel bands with 240 and 80 kDa, respectively [14]. In the present study, a somewhat higher molecular mass was obtained for the large subunit (293 +/− 11 kDa; n = 7) and a similar mass for the small subunit 83 +/− 6 kDa (n = 7), respectively. The amino acid sequence of the dLp/HDL–BGBP precursor was compared with the mass spectroscopic analysis of the two apoproteins of the dLp. 135 and 33 peptide fragments were found (supplementary Tables A3 and A4) with matches to the large (293 kDa) and the small (83 kDa) subunit of the dLp, respectively. In the small subunit, several fragments were found with matches to those in the large subunit which suggests the contamination of the corresponding band used for the mass spectroscopic analysis by degradation products of the large subunit. In contrast, no contaminating peptide fragments were found in the large subunit. The peptides specific for the large subunit were located on the N-terminal part of the dLp/HDL–BGBP precursor sequence while those specific for the small subunit were found C-terminal. The peptides sequence coverage was > 60% for either subunit. The peptide fragments were located adjacent to the two putative dibasic furin cleavage sites (RAKR and RARR, respectively; see Fig. 1) enclosing the HDL–BGBP sequence (see above) with a length of 1108 amino acids and a calculated molecular mass of 126 kDa.

For *M. rosenbergi*, the HDL–BGBP was also isolated, separated by SDS-PAGE and subjected to mass spectroscopic analysis as above. The peptide fragments (supplementary Table A6) showed matches to the HDL–BGBP sequence with sequence coverage of 68% and was also enclosed in two putative furin cleavage sites (RPRR and RVKR, respectively; see Fig. 1).

3.4. Hemolymph titers of dLp and HDL–BGBP in A. leptodactylus

The concentrations of dLp and HDL–BGBP were measured in the hemolymph showing levels between 1 and 6 mg/ml with no significant differences between sexes considering the sample variability (Fig. 3).

3.5. Isolation of an additional variant of the dLp in A. leptodactylus

During routine isolation of the dLp by ultracentrifugtion, some of our dLp preparations revealed a third apoprotein of 120 kDa as determined by SDS-PAGE analysis (Fig. 4).

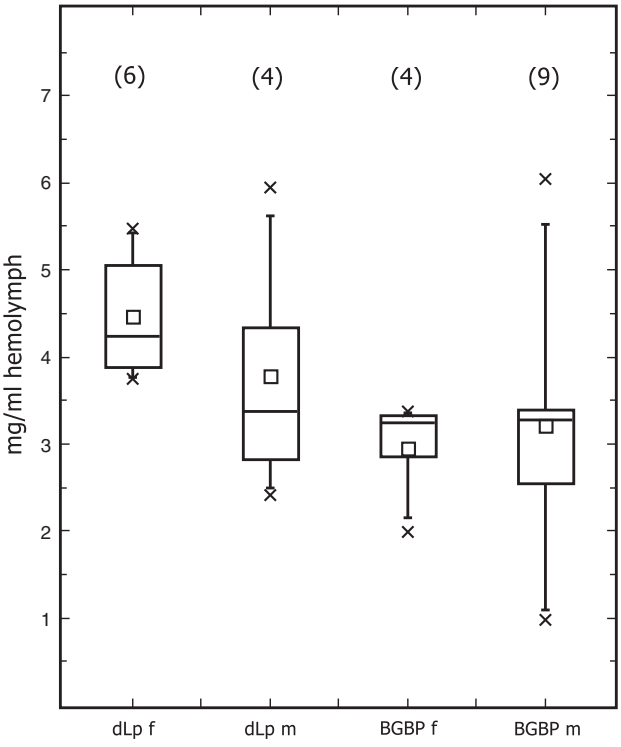

Fig. 3. Box plot of hemolymph titers (given as mg/ml hemolymph) of the discoidal lipoprotein (dLp) and the high density lipoprotein–β-glucan binding protein (HDL–BGBP) in female (f) and male (m) *A. leptodactylus*. The 25 and 75 percentile ranges are shown with mean values ( ), medians (—), minimal and maximal values (X). The number of measurements is given in parentheses.

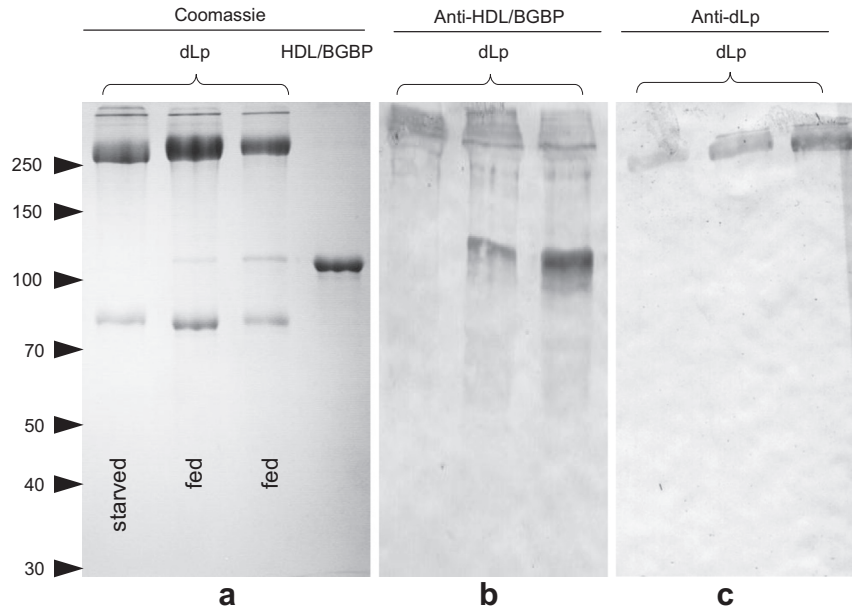

Fig. 4. Western blot staining of three preparations of the discoidal lipoprotein isolated from starved and fed *A. leptodactylus*. The Coomassie stained gel (a) shows dLp with and without a third 120 kDa apoprotein. The antiserum against HDL−β-glucan binding protein reacts with the 120 kDa apoprotein (b) while the antiserum against the discoidal lipoprotein reacts preferentially with the large subunit (293 kDa) of the discoidal lipoprotein (c).

Further investigations showed that the presence of this band was related to the feeding status of the animals. In animals starved for 6 weeks, the band was absent, while it was present in animals fed for 6 weeks with fish muscle ad libitum. The proportion of the 120 kDa apoprotein with respect to the other apoproteins was variable. The relative staining densities of the gel bands showed ratios close to unity for the 293 and 83 kDa apoproteins ($1.01 +/- 0.15$; $n = 6$), while the 120 kDa band had a lower relative density of only 0.1 to 0.3 of that of the other apoproteins (data not shown). Western blotting of the different dLp preparations showed that the 120 kDa apoprotein reacted preferentially with the antiserum against the β-glucan binding protein (Fig. 4b) while the other two apoproteins were preferentially reactive with the antiserum against the large subunit of the dLp (Fig. 4c). The 120 kDa apoprotein contained in the dLp however was larger than the apoprotein of the BGBP of *A. leptodactylus* (105 kDa) as determined by gel band analysis (Fig. 3a). The analysis of the 120 kDa apoprotein by mass spectroscopic analysis was carried out as above. For two preparations, 42 and 46 peptides, respectively, were identified (see supplementary Table A5) matching the sequence of the HDL–BGBP with a sequence coverage of 53 and 60%, respectively. As with the small dLp subunit (see above), contaminating peptides were present which could be assigned to the large and the small subunit of the dLp suggesting the presence of degradation products and/or aggregates in this band.

3.6. Immunohistochemical staining of hepatopancreas tissue and cells

Immunohistochemical staining of the hepatopancreatic tubules in *A. leptodactylus* revealed labeling of all cell types (Fig. 5a). Labeling was especially evident on the cell border facing the luminal side of the tubulus. In isolated hepatopancreas cells (Fig. 5b), staining was evident as small vesicle like structures of 0.2–0.4 μm diameter.

4. Discussion

Due to its unusually large size, its discoidal shape and its occurrence, in a strikingly similar way, in two remote invertebrates, the crayfish *A. leptodactylus* [14] and the polychaete *N. virens* [5], we speculated that the large discoidal lipoproteins might represent a prototype class of lipoproteins [14]. The present study also opened up the opportunity to study for the first time the relationship of BGBP with other lipoprotein families showing by both transcriptome and combined MS peptide and tandem MS fragmentation analysis that the dLp and the BGBP are related in that they arise from a large common precursor peptide.

4.1. Structure of the dLp/HDL–BGBP precursor

The presence of a N-terminal lipid binding domain places the large dLp subunit of *A. leptodactylus* in the family of the apoB-type, large lipid transfer proteins which includes insect apolipophorin-I/II, vitellogenin, microsomal triglyceride transfer protein [37] and more recently, insect lipid transfer particle [38]. The same domain architecture was found also for *M. rosenbergii* in which the large subunit contains two domains of unknown functions, DUF 1943 (Pfam 09172 motif) and DUF 1081 (Pfam 06448 motif) showing that the results of the present study do not represent an isolated instance. The DUF 1081 motif is found in ApoB type lipoproteins and in the crustacean yolk proteins. The latter are related to the ApoB type lipoproteins and not to the "classical" vitellogenins, and therefore, the term "apolipocrustacein" has been introduced to avoid confusion [39]. In contrast, the "classical" vitellogenins of insects and vertebrates and crustacean clotting proteins lack DUF 1081. Although the apolipocrustacein of *A. leptodactylus* has not been sequenced yet, a similar structure can be expected as in other decapods (see [30]). Thus, our findings indicate that at least *A. leptodactylus, A. astacus* and *M. rosenbergii* contain two ApoB type lipoproteins, one female specific (i.e., apolipocrustacein) and one sex unspecific (i.e., dLp), and this is likely to be true for other decapod crustaceans given the similarity of the sequences found in other species (see Fig. 2).

4.2. Relationship of the discoidal lipoprotein with the Crustacean high density lipoprotein/β-glucan binding protein

A striking feature of the *A. leptodactylus* dLp/HDL–BGBP precursor is the presence of two dibasic furin type cleavage sites (RAKR and RARR, respectively) which enclose the sequence of the HDL–BGBP. Corresponding cleavage sites are present in *M. rosenbergii* (RPRR and RVKR,

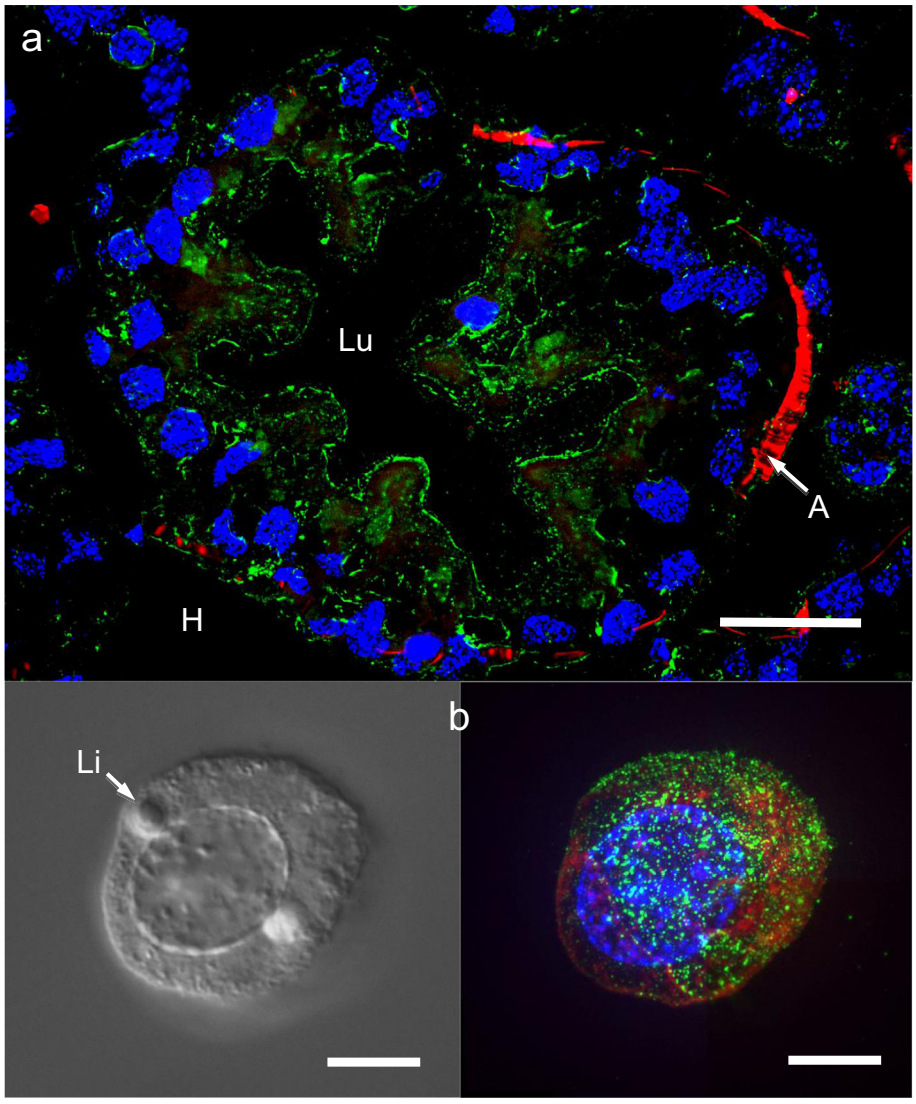

Fig. 5. Immunohistochemical staining of the hepatopancreas tissue of *A. leptodactylus* using antiserum against the discoidal lipoprotein. (5a) Cross section of a hepatopancreas tubule; the labeling of the cell borders is evident (Atto 647 fluorescence, pseudocolored green). 5b, light microscopical (left) and fluorescent image (right) of an isolated hepatopancreas cell (Atto 488; green fluorescence). The red fluorescence indicates labeling of the actin cytoskeleton using TRITC-phalloidin. Nuclei are shown in blue (DAPI staining). A, actin labeling of a muscle fiber surrounding the hepatopancreas tubule, Lu, tubule lumen, H, hemolymph space surrounding the tubule, Li, lipid droplet. Scale bars 50 μm (5a), 10 μm (5b).

respectively; see Fig. 1) and they have also been found in the BGBP/HDL's of two penaeid shrimps (RSKR and RVRR, respectively; see Fig. 2) as well as in three translated EST's as predicted by the ProP online tool.

It has been noted before [23,24] that the translated sequences of HDL–BGBPs in two other crustaceans exceed those of the mature protein circulating in the hemolymph which have molecular masses between 100 and 110 kDa ([13] and cited references); [14]. In *P. leniusculus*, a C- and N-terminal processing has been suggested [23]. The possible processing by furin cleavage has been proposed [24]. This is supported by our study on *A. leptodactylus* and by the comparison with several related sequences published for the HDL–BGBP which show the same two potential convertase cleavage sites with a dibasic motif (see Fig. 3). The novel finding of our study, however, is the transcriptomic location of HDL–BGBP between the two dLp subunits, forming a large common precursor for both proteins. Our results can thus serve to explain the apparent discrepancy between the calculated molecular masses of the published sequences for the HDL–BGBP and the molecular mass of the mature HDL–BGBP [20,23,24]. These findings would then be consistent with our view that both the two subunits of the dLp and the HDL–BGBP arise from processing of this large precursor by a furin type protease leading to the release of the large subunit of the dLp from the N-terminal side, the central part to form the mature BGBP and the small subunit of the dLp from the C-terminal side. The two dLp subunits would then assemble to form the dLp holoparticle with a 1:1 stoichiometry as suggested by the gel band densitometry while the HDL–BGBP forms a homodimer as found before through crosslinking experiments [14].

The sorting mechanisms leading to the formation of the two different lipoproteins BGBP and dLp from the large precursor peptide are still unknown. Lipophorin, the major hemolymph lipoprotein in insects, originates as a single precursor peptide and is also cleaved by a furin like protease yielding two apolipoproteins, apoLp I and apoLp II [40,41]. In a Crustacean vitellogenin, even three furin type cleavage sites have been identified [42]. The processing of a large precursor protein by two potential furin cleavage sites resulting in the formation of the dLp heterodimer and the BGBP homodimer seems unique and has not been reported in arthropods.

With respect to the assembly of the native dLp and BGBP this leads to an interesting speculation. As lipidation of the nascent particle usually

occurs in parallel to the peptide backbone biosynthesis [8,43,44], and, in the case of the insect lipophorins, furin mediated cleavage of the apolipophorin-II/I-precursor takes place posttranslationally [8,43] this would imply that also HDL–BGBP is lipidated along with dLp and "cut out" of dLp posttranslationally. However, if the released HDL–BGBP then remains in the ER (associated with the ER-membrane) and then combines with a second HDL–BGBP monomer, or if it is secreted in a low-lipidation state and extracellularly associates with another low lipidated BGBP just as in the nascent vertebrate HDL [45] remains elusive.

If our view is correct, the hypothetical precursor peptide in *A. leptodactylus* is expected to have a theoretical molecular mass of about 502 kDa (293 + 126 + 83 kDa). In contrast, the calculated molecular mass of the dLp/HDL–BGBP precursor from the open reading frame obtained from Illumina sequencing gives a value of 546 kDa. This may be attributable to an additional processing of the large dLp subunit, since for the small subunit, the calculated molecular mass (83 kDa) agrees well with that obtained from the gel band analysis (80 kDa). The central part of the dLp/HDL–BGBP precursor, representing the HDL–BGBP, translates to a molecular mass of 126 KDa which is larger than the HDL–BGBP of both *A. leptodactylus* and *A. astacus* (105 kDa; [14]) as well as that of the HDL–BGBP in other species [6,12]. Therefore, the mature BGBP could likewise arise by further processing following the furin cleavage by a yet unknown protease.

Measurements of the hemolymph titers of the two lipoproteins in *A. leptodactylus* (see Fig. 3) show that the levels are in the same range (1-6 mg/ml hemolymph) with a trend to higher values for the dLp. However, the levels are rather variable which precludes the judgment of the stoichiometry in the hemolymph. The hemolymph was sampled between June and Sept which covers different phases of vitellogenesis/spermatogenesis which starts in June in *A. leptodactylus* [46]. The observed variations in the titers of the two lipoproteins could thus be influenced by different phases of the reproductive cycle which was not investigated in our study. If both lipoproteins originate from a common precursor, one holoparticle of dLp and 0.5 particle of HDL–BGBP may be formed after lipidation of the apoproteins assuming a homodimeric structure of HDL–BGBP. Considering a molecular mass of 376 kDa (293 + 83) for the large and small subunit, respectively, and a molecular mass of 105 kDa for the HDL–BGBP, this would call for a more than three-fold excess for the dLp over the HDL–BGBP in the hemolymph on a protein basis if both proteins are released in equimolar amounts. This was clearly not observed and may indicate that not all of the dLp peptides are released into the hemolymph after translation. Such a situation exists in vertebrate (rat) ApoB-100, where part of the translated peptides are subjected to ER-associated degradation and reuptake [47] thus leading to their reduced secretion. Alternatively, an unproportional removal of the dLp from the hemolymph could also contribute to these apparent discrepancies. For instance, unpublished immunohistochemical data indicate the presence of dLp in hemocytes of *A. leptodactylus* and several other decapod crustaceans suggesting these cells as a possible sink for dLp.

4.3. The presence of a BGBP like apoprotein in the mature dLp

In fed animals, isolation of the dLp using gradient density ultracentrifugation revealed a dLp containing three instead of two apoproteins (see Fig. 4a). The additional apoprotein was reactive against the HDL–BGBP antibody (see Fig. 4b) while the antiserum against the dLp preferentially marked the large subunit of the dLp (Fig. 4c). Gel band analysis of this apoprotein showed a molecular mass of 120 kDa and in comparison, calculation of the amino acid sequence of HDL–BGBP enclosed by the putative furin cleavage sites shows a similar calculated molecular mass of 126 kDa. When this apoprotein band was subjected to mass spectroscopic analysis, the peptide fragments obtained matched those of the HDL–BGBP sequence. The presence of a third apoprotein in the dLp with properties similar to the HDL–BGBP indicates that the processing of the large dLp/HDL–BGBP precursor peptide may lead to incomplete separation of the cleavage products resulting in the incorporation of the HDL–BGBP apoprotein in the assembled dLp particle. The 293 and 83 kDa band always exhibited a stoichiometry close to unity while the relative density of the 120 kDa band was variable (see Results). This indicates that not all of the lipoprotein particles may contain the third apoprotein and that assembly of these additional dLp variants proceeds with a variable stoichiometry with respect to the HDL–BGBP content. We considered the possibility that the 120 kDa band could represent an independent HDL–BGBP lipoprotein with a higher degree of lipidation and a buoyant density identical to that of the dLp so that both proteins would be recovered in the same fraction. The dLp preparations from fed and starved animals were separated by gel filtration applying the same conditions used earlier for the separation and molecular weight determination of the HDL/BGBP and the dLp. Both proteins show different molecular masses due to their large differences in apoprotein composition and their degree of lipidation [14]. However, no separation in two different lipoprotein fractions (i.e., a dLp and a HDL–BGBP fraction) was observed (unpublished data), indicating that the 120 kDa apoprotein was associated with the dLp particle.

4.4. Immunohistochemical localization of the dLp in A. leptodactylus

On the cellular level, we have demonstrated the localization of the dLp in the hepatopancreas as a major site of lipoprotein biosynthesis as previously demonstrated for the HDL–BGBP in a shrimp [48]. The dLp localization was especially visible in the apical cell border facing the lumen of the hepatopancreatic tubule. Since the dLp as well as the HDL–BGBP can be assumed to be exported into the surrounding hemolymph space this finding may indicate that dLp synthesis takes place directly after the uptake of lipid precursors from the digestive fluid into the hepatopancreatic cells. The labeling of the dLp could also be a result of reuptake of the synthesized lipoproteins depending on the nutritional status of the animal.

4.5. Occurrence of discoidal lipoprotein related proteins in other crustaceans and possible functions

We had previously found the discoidal lipoprotein in *A. leptodactylus* only and attempts to isolate similar proteins from the hemolymph of the congener, *A. astacus,* and several other decapods have failed so far ([14] and unpublished results). On the other hand, the identification of the sequence of a related protein in *A. astacus*, the prawn *M. rosenbergii* and the comparison with existing Genbank entries and EST sequences (see Fig. 2) do suggest that dLp like proteins are widely spread among Crustaceans. This discrepancy could be explained by a lower rate of synthesis or secretion of the dLp into the hemolymph compared to the HDL–BGBP in other species. However, this seems unlikely. If both the dLp and the HDL–BGBP originate from a common precursor peptide with subsequent proteolytic processing, both lipoproteins should be present in the hemolymph in similar concentration ranges even taking differences in the release rates (see above) into account. In *A. leptodactylus*, our ELISA measurements indicate that both the dLp and the HDL–BGBP occur in the hemolymph in comparable concentrations (see Fig. 3). As an alternative explanation, our isolation procedure which involves flotation on KBr gradients would fail for low and non lipidated dLp like proteins. These unlipidated proteins would have to be isolated from the hemolymph by alternative methods such as antibody affinity columns. Current experiments are on the way to tackle this problem. The high lipid binding capacity thus seems unique for the dLp of *A. leptodactylus* so far and remains enigmatic.

Recently, Sun et al. [49] have found that a recombinant DUF 1943 domain derived from zebra fish vitellogenin is able to bind to several gram positive and negative bacteria as well as to lipopolysaccharides thus acting as a pattern recognition protein. In this light, the presence of the DUF 1943 domain in the dLp would suggest a function of the dLp and related

proteins in innate immune system working in concert with the known functions of the HDL–BGBP and LP–BGBP in the defensive system of crustaceans (see [50] for a review). Such an important function would call indeed for a widespread presence of dLp related proteins at least in the decapod crustaceans.

Acknowledgments

This study was supported in part by a grant from the Feldbausch Foundation (Hoeger 2014) at the University of Mainz to U.H. and B.L.

Appendix A. Supplementary data

Supplementary data to this article can be found online at http://dx.doi.org/10.1016/j.bbalip.2014.09.020.

References

[1] D. Rhainds, L. Brissette, Low density lipoprotein uptake: holoparticle and cholesteryl ester selective uptake, Int. J. Biochem. Cell Biol. 31 (1999) 915–931.
[2] N.H. Haunerland, W.S. Bowers, Lipoproteins in the hemolymph of the tarantula, *Eurypelma californicum*, Comp. Biochem. Physiol. B 86 (1987) 571–574.
[3] K.W. Rodenburg, D.J. van der Horst, Lipoprotein-mediated lipid transport in insects: Analogy to the mammalian lipid carrier system and novel concepts for the functioning of LDL receptor family members, Biochim. Biophys. Acta 1736 (2005) 10–29.
[4] S. Schenk, H. Gras, D. Marksteiner, L. Patasic, B. Prommnitz, U. Hoeger, The *Pandinus imperator* haemolymph lipoprotein, an unusual phosphatidylserine carrying lipoprotein, Insect Biochem. Mol. Biol. 39 (2009) 735–744.
[5] S. Schenk, J.R. Harris, U. Hoeger, A discoidal lipoprotein from the coelomic fluid of the polychaete *Nereis virens*, Comp. Biochem. Physiol. B 143 (2006) 236–243.
[6] M. Hall, M.C. van Heusden, K. Söderhäll, Identification of the major lipoproteins in crayfish hemolymph as proteins involved in immune recognition and clotting, Biochem. Biophys. Res. Commun. 216 (1995) 939–946.
[7] M. Hall, R. Wang, R. van Antwerpen, l. Sotterup-Jensen, K. Söderhäll, The crayfish plasma clotting protein: a vitellogenin-related protein responsible for clot formation in crustacean blood. Proc. Natl. Acad. Sci. U. S. A. 96 (1999) 1965–1970.
[8] M.M. Smolenaars, M.A. Kasperaitis, P.E. Richardson, K.W. Rodenburg, D.J. Van der Horst, Biosynthesis and secretion of insect lipoprotein: involvement of furin in cleavage of the apoB homolog, apolipophorin-II/I, J. Lipid Res. 46 (2005) 412–421.
[9] E. Spaziani, R.J. Havel, R.L. Hamilton, D.A. Hardman, J.B. Stoudemire, R.D. Watson, Properties of serum high-density lipoproteins in the crab, *Cancer antennarius* Stimpson, Comp. Biochem. Physiol. B 85 (1986) 307–314.
[10] G.M. Yepiz-Plascencia, R. Sotelo-Mundo, L. Vazquez-Moreno, R. Ziegler, I. Higuera-Ciapara, A non-sex-specific hemolymph lipoprotein from the white shrimp *Penaeus vannamei* Boone. Isolation and partial characterization. Comp. Biochem. Physiol. B 111 (1995) 181–187.
[11] E. Lubzens, T. Ravid, M. Khayat, N. Daube, A. Tietz, Isolation and characterization of the high-density lipoproteins from the hemolymph and ovary of the penaeid shrimp *Penaeus semisulcatus* (de Haan): apoproteins and lipids, J. Exp. Zool. 278 (1997) 339–348.
[12] L.M. Ruiz-Verdugo, M.L. García-Bañuelos, F. Vargas-Albores, H.-C. Inocencio, G.M. Yepiz-Plascencia, Amino acids and lipids of the plasma HDL from the white shrimp *Penaeus vannamei* Boone, Comp. Biochem. Physiol. B 118 (1997) 91–96.
[13] G.M. Yepiz-Plascencia, T. Gollas Galván, F. Vargas-Albores, M.L. García-Bañuelos, Synthesis of hemolymph high-density lipoprotein ß-glucan binding protein by *Penaeus vannamei* shrimp hepatopancreas, Mar. Biotechnol. 2 (2000) 485–492.
[14] S. Stieb, U. Hoeger, S. Schenk, A large discoidal lipoprotein present in only one of two closely related crayfish, J. Comp. Physiol. B. 178 (2008) 755–765.
[15] J.M. Kollman, J. Quispe, The 17 Å structure of the 420 kDa lobster clottable protein by single particle reconstruction from cryoelectron micrographs, J. Struct. Biol. 151 (2005) 306–314.
[16] L.M. Perazzolo, D.M. Lorenzini, S. Daffre, M.A. Barracco, Purification and partial characterization of the plasma clotting protein from the pink shrimp *Farfantepenaeus paulensis*, Comp. Biochem. Physiol. B 142 (2005) 302–307.
[17] P. Jiravanichpaisal, B.L. Lee, K. Soderhall, Cell-mediated immunity in arthropods: hematopoiesis, coagulation, melanization and opsonization, Immunobiology 211 (2006) 213–236.
[18] L. Cerenius, K. Söderhäll, Coagulation in invertebrates, J. Innate Immun. 3 (2011) 3–8.
[19] B. Duvic, K. Söderhäll, Purification and partial characterization of a beta-1,3-glucan-binding-protein membrane receptor from blood cells of the crayfish *Pacifastacus leniusculus*, Eur. J. Biochem. 207 (1992) 223–228.
[20] X. Lai, J. Kong, Q. Wang, W. Wang, X. Meng, Cloning and characterization of a beta-1,3-glucan-binding protein from shrimp *Fenneropenaeus chinensis*, Mol. Biol. Rep. 38 (2011) 4527–4535.
[21] D. Zhao, L. Chen, C. Qin, H. Zhang, P. Wu, E. Li, L. Chen, J. Qin, Molecular cloning and characterization of the lipopolysaccharide and beta-1, 3-glucan binding protein in Chinese mitten crab (*Eriocheir sinensis*), Comp. Biochem. Physiol. B 154 (2009) 17–24.
[22] B. Zeis, T. Lamkemeyer, R.J. Paul, F. Nunes, S. Schwerin, M. Koch, W. Schutz, J. Madlung, C. Fladerer, R. Pirow, Acclimatory responses of the *Daphnia pulex* proteome to environmental changes. I. Chronic exposure to hypoxia affects the oxygen transport system and carbohydrate metabolism, BMC Physiol. 9 (2009) 7.
[23] L. Cerenius, Z. Liang, B. Duvic, P. Keyser, U. Hellman, E.T. Palva, S. Iwananga, K. Söderhäll, Structure and biological activity of a 1,3-ß-D-glucan-binding protein in crustacean blood, J. Biol. Chem. 269 (1994) 29462–29467.
[24] M.G. Romo-Figueroa, C. Vargas-Requena, R.R. Sotelo-Mundo, F. Vargas-Albores, I. Higuera-Ciapara, K. Soderhall, G. Yepiz-Plascencia, Molecular cloning of a beta-glucan pattern-recognition lipoprotein from the white shrimp *Penaeus* (*Litopenaeus*) *vannamei*: correlations between the deduced amino acid sequence and the native protein structure, Dev. Comp. Immunol. 28 (2004) 713–726.
[25] D.A. Bricarello, J.T. Smilowitz, A.M. Zivkovic, J.B. German, A.N. Parikh, Reconstituted lipoprotein: a versatile class of biologically-inspired nanostructures, ACS Nano 5 (2011) 42–57.
[26] R.L. Hamilton, M.C. Williams, C.J. Fielding, R.J. Havel, Discoidal bilayer structure of nascent high density lipoproteins from perfused rat liver, J. Clin. Invest. 58 (1976) 667–680.
[27] J. Babiak, H. Tamachi, F.L. Johnson, J.S. Parks, L.L. Rudel, Lecithin: cholesterol acyltransferase-induced modifications of liver perfusate discoidal high density lipoproteins from African green monkeys, J. Lipid Res. 27 (1986) 1304–1317.
[28] P. Chomczynski, N. Sacchi, Single-step method of RNA isolation by acid guanidinium thiocyanate-phenol-chloroform extraction, Anal. Biochem. 162 (1987) 156–159.
[29] T. Ventura, R. Manor, E.D. Aflalo, V. Chalifa-Caspi, S. Weil, O. Sharabi, A. Sagi, Post-embryonic transcriptomes of the prawn *Macrobrachium rosenbergii*: multigenic succession through metamorphosis, PLoS One 8 (2013) e55322.
[30] Z. Roth, S. Parnes, S. Weil, A. Sagi, N. Zmora, J. Chung, I. Khalaila, N-glycan moieties of the crustacean egg yolk protein and their glycosylation sites, Glycoconj. J. 27 (2010) 159–169.
[31] J. Kyhse-Andersen, Electroblotting of multiple gels: a simple apparatus without buffer tank for rapid transfer of proteins from polyacrylamide to nitrocellulose, J. Biochem. Biophys. Methods 10 (1984) 203–209.
[32] M. Blake, A rapid, sensitive method for detektion of alkaline phosphatase-conjugated anti-antibody on Western blots, Anal. Biochem. 136 (1984) 175–179.
[33] L. Fiandra, P.K. Mandal, B. Giordana, G.A. Ahearn, L-proline transport by purified cell types of lobster hepatopancreas, J. Exp. Zool. A 305 (2006) 851–861.
[34] P. Duckert, S. Brunak, N. Blom, Prediction of proprotein convertase cleavage sites, Protein Eng. Des. Sel. 17 (2004) 107–112.
[35] T.N. Petersen, S. Brunak, G. von Heijne, H. Nielsen, SignalP 4.0: discriminating signal peptides from transmembrane regions, Nat. Methods 8 (2011) 785–786.
[36] L.A. Kelley, M.J. Sternberg, Protein structure prediction on the Web: a case study using the Phyre server, Nat. Protoc. 4 (2009) 363–371.
[37] M.M.W. Smolenaars, O. Madsen, K.W. Rodenburg, D.J. Van der Horst, Molecular diversity of the large lipid transfer protein superfamily, J. Lipid Res. 48 (2007) 489–502.
[38] H. Yokoyama, T. Yokoyama, M. Yuasa, H. Fujimoto, T. Sakudoh, N. Honda, H. Fugo, K. Tsuchida, Lipid transfer particle from the silkworm, *Bombyx mori*, is a novel member of the apoB/large lipid transfer protein family, J. Lipid Res. 54 (2013) 2379–2390.
[39] J.-C. Avarre, E. Lubzens, P.J. Babin, Apolipocrustacein, formerly vitellogenin, is the major egg yolk precursor protein in decapod crustaceans and is homologous to insect apolipophorin II/I and vertebrate apolipoprotein B, BMC Evol. Biol. 7 (2007).
[40] P.M. Weers, W.J. Van Marrewijk, A.M. Beenakkers, D.J. Van der Horst, Biosynthesis of locust lipophorin. Apolipophorins I and II originate from a common precursor, J. Biol. Chem. 268 (1993) 4300–4303.
[41] M.M.W. Smolenaars, M.A.M. Kasperaitis, P.E. Richardson, K.W. Rodenburg, D.J. Van der Horst, Biosynthesis and secretion of insect lipoprotein: involvement of furin in cleavage of the apoB homolog, apolipophorin-II/I, J. Lipid Res. 46 (2005) 412–421.
[42] A. Okuno, W.J. Yang, V. Jayasankar, H. Saido-Sakanaka, D.T. Huong, S. Jasmani, M. Atmomarsono, T. Subramoniam, N. Tsutsui, T. Ohira, I. Kawazoe, K. Aida, M.N. Wilder, Deduced primary structure of vitellogenin in the giant freshwater prawn, *Macrobrachium rosenbergii*, and yolk processing during ovarian maturation, J. Exp. Zool. 292 (2002) 417–429.
[43] P.M.M. Weers, D.J. van der Horst, W.J.A. van Marrewijk, M. van den Eijnden, J.M. van Doorn, A.M.T. Beenakkers, Biosynthesis and secretion of insect lipoprotein, J. Lipid Res. 33 (1992) 485–491.
[44] V. Gusarova, J.L. Brodsky, E.A. Fisher, Apolipoprotein B100 exit from the endoplasmatic reticulum (ER) is COPII-dependent, and its lipidation to very low density lipoprotein occurs post-ER, J. Biol. Chem. 278 (2003) 48051–48058.
[45] P.E. Fielding, C.J. Fielding, Plasma membrane calveolae mediate the efflux of cellular free cholesterol, Biochemistry 34 (1995) 14288–14292.
[46] S.M. Mirheydari, A. Matinfar, M. Soltani, A. Kamali, Y.A. Asadpour-Ousalou, S. Safi, M. Paolucci, Fluctuation of gonadosomatic index during oocyte development in the narrow-clawed crayfish *Astacus leptodactylus* (Eschscholtz, 1823) in Aras Dam Lake, Iran, Iran. J. Fish. Sci. 13 (2014) 103–111.
[47] E.A. Fisher, M. Pan, X. Chen, X. Wu, H. Wang, H. Jamil, J.D. Sparks, K.J. Williams, The triple threat to nascent apolipoprotein B evidence for multible, distinct degradative pathways, J. Biol. Chem. 276 (2001) 27855–27863.
[48] A. Muhlia-Almazan, A. Sanchez-Paz, F. Garcia-Carreno, A.B. Peregrino-Uriarte, G. Yepiz-Plascencia, Starvation and diet composition affect mRNA levels of the high density-lipoprotein-beta glucan binding protein in the shrimp *Litopenaeus vannamei*, Comp. Biochem. Physiol. B 142 (2005) 209–216.
[49] C. Sun, L. Hu, S. Liu, Z. Gao, S. Zhang, Functional analysis of domain of unknown function (DUF) 1943, DUF1944 and von Willebrand factor type D domain (VWD) in vitellogenin2 in zebrafish, Dev. Comp. Immunol. 41 (2013) 469–476.
[50] O. Schmidt, K. Soderhall, U. Theopold, I. Faye, Role of adhesion in arthropod immune recognition, Annu. Rev. Entomol. 55 (2010) 485–504.